催 化 学 报
2010 Chinese Journal of Catalysis Vol. 31 No. 10

文章编号: 0253-9837(2010)10-1233-09 国际版 DOI: 10.1016/S1872-2067(10)60117-9 研究论文: 1233~1241

# 高硅Na-ZSM-5分子筛表面NO的常温吸附-氧化机理

刘华彦[1,2], 张泽凯[2], 徐媛媛[2], 陈银飞[2], 李 希[1]

[1]浙江大学化学工程与生物工程系, 浙江杭州 310027

[2]浙江工业大学化学工程与材料学院, 浙江杭州 310014

**摘要:** 采用程序升温表面反应(TPSR)和原位漫反射红外光谱(DRIFTS)等手段研究了常温下NO和$O_2$在高硅Na-ZSM-5分子筛上吸附-氧化反应机理. 结果表明, Na-ZSM-5分子筛上NO的催化氧化过程中伴随着显著的$NO_2$物理吸附, 表现为NO氧化和$NO_2$吸附间的动态平衡. Na-ZSM-5分子筛表面$NO_x$吸附物种的TPSR和原位DRIFTS表征表明, 化学吸附的NO和气相中的$O_2$在Na-ZSM-5表面反应生成吸附态的$NO_3$, 并继续与NO作用生成弱吸附的$NO_2$和$N_2O_4$, 它们吸附饱和后释放出来; 其中, 强吸附的$NO_3$在NO氧化过程中起到了反应中间体的作用, 同时也促进了NO的吸附.

**关键词:** Na-ZSM-5分子筛; 一氧化氮; 氧化; 氮氧化物; 吸附; 脱除

**中图分类号:** O643/X7 **文献标识码:** A

# Adsorption-Oxidation Reaction Mechanism of NO on Na-ZSM-5 Molecular Sieves with a High Si/Al Ratio at Ambient Temperature

LIU Huayan[1,2], ZHANG Zekai[2], XU Yuanyuan[2], CHEN Yinfei[2,*], LI Xi[1]

[1]*Department of Chemical and Biological Engineering, Zhejiang University, Hangzhou 310027, Zhejiang, China*

[2]*College of Chemical Engineering and Materials Science, Zhejiang University of Technology, Hangzhou 310014, Zhejiang, China*

**Abstract:** The oxidation reaction mechanism of NO by $O_2$ over Na-ZSM-5 molecular sieves with a high $SiO_2/Al_2O_3$ ratio was studied at ambient temperature by temperature-programmed surface reaction (TPSR) and in situ diffuse reflectance infrared Fourier transform spectroscopy (DRIFTS). The results show that the NO catalytic oxidation process is accompanied by a significant adsorption of $NO_2$ and it exhibits a dynamic equilibrium between $NO_2$ adsorption and the reaction of NO. TPSR and in situ DRIFTS characterization of the adsorbed $NO_x$ species revealed that adsorbed $NO_3$ formed on the surface of the Na-ZSM-5 molecular sieve as a result of the reaction between adsorbed NO and gaseous $O_2$. The oxidation of $NO_3$ with NO produced weakly-adsorbing $NO_2$ and $N_2O_4$ which were released once the adsorption reached saturation. Therefore, the strongly-adsorbing $NO_3$ was an intermediate of the NO oxidation reaction and its presence promoted NO adsorption.

**Key words:** Na-ZSM-5 molecular sieve; nitric oxide; oxidation; nitrogen oxide; adsorption; removal

氮氧化物($NO_x$)对生态环境和人类健康造成极大的危害, 脱除$NO_x$成为当前环境领域的重要研究课题之一. 选择性催化还原法(SCR)、液体吸收法和吸附法是当前应用最广泛的技术, 这三种方法的处理效果都与$NO_x$中$NO_2$的含量有关. Goo等[1]发现在$V_2O_5$-$WO_3$-$MnO_2/TiO_2$上的$NH_3$-SCR过程中, 提高$NO_2$含量可大大降低反应温度, 最佳$NO_2$:$NO_x$比为0.5; Koebel等[2]指出, 当$NO_2$:NO为1:1时在$V_2O_5$-$WO_3/TiO_2$上SCR活性最高. 而在碱液吸收法中要得到高的$NO_x$脱除率, 也必须提高$NO_2$的含量. 当采用NaOH溶液吸收, 则需$NO_2$:$NO_x$比为0.5~0.6[3~5]; 若采用$(NH_4)_2SO_3$-NaOH等还原性碱液吸收, 所需要的$NO_2$:$NO_x$比更高[6]. 在吸附法中由于NO难吸附, 只有将NO氧化成$NO_2$才能获得较高的吸附量[7]. 因

收稿日期: 2010-04-02.

联系人: 陈银飞. Tel: (0571)88320622; Fax: (0571)88320544; E-mail: yfchen@zjut.edu.cn

基金来源: 浙江省科技厅资助项目(2007C23034).

本文的英文电子版由Elsevier出版社在ScienceDirect上出版(http://www.sciencedirect.com/science/journal/18722067).

此, 如何将 $NO_x$ 废气中占 90% 以上的 NO[8] 部分氧化成 $NO_2$ 以提高 $NO_x$ 脱除率, 是上述处理工艺共有的关键问题.

ZSM-5 分子筛及金属离子交换的 ZSM-5 应用于 $NO_x$ 吸附和还原的研究较多[9,10], 而有关以高硅 ZSM-5 为常温 NO 氧化催化剂鲜有报道. 针对活性炭和活性炭纤维在常温含水汽环境下氧化活性低[11]的缺点, 我们重点研究了高硅 ZSM-5 分子筛催化氧化 NO 性能, 发现该催化剂在高水汽含量气氛下具有远高于活性炭等材料的低温催化氧化活性[12], 可望实现工业化应用. 因此, 本文进一步研究高硅 Na-ZSM-5 分子筛上 NO 和 $O_2$ 的反应过程及表面吸附物种, 探讨 NO 常温吸附-氧化反应机理, 以期对后续的催化剂改进和反应动力学研究等提供理论指导.

## 1 实验部分

### 1.1 催化剂处理及活性评价

Na-ZSM-5 ($SiO_2/Al_2O_3$ = 300) 由上海卓悦化工有限公司提供. 分子筛原粉的处理及活性评价方法参见文献[12]. 反应条件: 催化剂装填量为 3.7 g, 反应气体积分数为 0.05% NO, 20.7% $O_2$, $N_2$ 平衡; 气体总流量 2 L/min, 反应温度 30 °C. 使用 Testo 350-XL 型烟气分析仪测定 NO 和 $NO_2$ 进出口浓度.

### 1.2 催化剂表征

在进行程序升温表面反应 (TPSR) 时, 将 Na-ZSM-5 分子筛先于 500 °C, $N_2$ 气中吹扫 2 h 后冷至 30 °C, 将 $N_2$ 切换成 20.7% $O_2$-79.3% $N_2$, 0.05% NO-99.95% $N_2$, 0.05% NO-20.7% $O_2$-79.25% $N_2$ 或 0.05% $NO_2$-99.95% $N_2$ 等不同的混合气进行吸附. 出口气体浓度用烟气分析仪检测. 吸附饱和后用 $N_2$ 吹扫, 以除去表面上可逆吸附或弱吸附组分. 然后在 He 气 (20 ml/min) 中以 10 °C/min 从 30 °C 程序升温至 600 °C, 用 Omini Star 型质谱仪检测脱附物种.

在进行原位漫反射红外光谱 (DRIFTS) 测试时, 采用 VENTEX 70 型红外光谱仪进行 Na-ZSM-5 分子筛上 NO 和 $O_2$ 反应, MCT 检测器, 分辨率为 4 $cm^{-1}$, 扫描 128 次. 把粉末状 ZSM-5 分子筛样品装入漫反射原位池中, 装满刮平, 在 400 °C 用 $N_2$ 气 (100 ml/min) 吹扫 2 h 后将原位池冷却到设定温度, 测定不同温度下试样上未吸附反应物的 DRIFTS 谱, 将其作为相同温度下吸附反应物后的背景, 然后通入各种组成的混合气进行吸附-反应, 并适时记录谱图.

## 2 结果与讨论

### 2.1 Na-ZSM-5 分子筛催化氧化 NO 瞬态反应研究

图 1 为 NO 和 $O_2$ 流经高硅 Na-ZSM-5 催化剂床层后出口 NO 和 $NO_2$ 浓度随时间的变化. 由图可见, 通入 NO 后很短的时间内出口就出现 NO, 但浓度低于进口, 说明发生了 NO 的吸附, 而出口 $NO_2$ 浓度极低. 随着时间的延长, 出口 NO 浓度不断增加, 到 60 min 后, 其浓度急剧减少, 而 $NO_2$ 浓度快速增加, 至 65 min 后达到稳定状态, 进出口 $NO_x$ 浓度平衡. 在相同条件下进行了空白实验, 发现在 5 min 内即可稳定, 出口 NO 浓度为 0.0497%, NO 的氧化可忽略, 而在装填 Na-ZSM-5 的反应器中有大量 $NO_2$ 生成, 表明 Na-ZSM-5 确实起到了催化剂的作用.

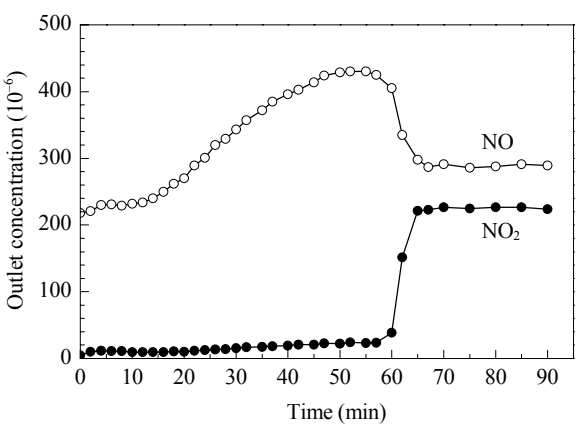


**图 1 NO 在 Na-ZSM-5 上氧化反应瞬态变化曲线**

**Fig. 1.** Transient NO oxidation profiles on Na-ZSM-5. Reaction conditions: NO 0.05%, $O_2$ 20.7%, $N_2$ balance, 30 °C.

### 2.2 Na-ZSM-5 分子筛上 NO 氧化反应体系的 TPSR 研究

图 2 是 Na-ZSM-5 单独吸附 $O_2$ 后的 TPSR 谱. 可以发现, 并未出现 $O_2$ 脱附峰, 说明 $O_2$ 在 Na-ZSM-5 上是不吸附的. 图 3 为 Na-ZSM-5 饱和吸附不同组成混合气后的 TPSR 谱. 其中图 3(a) 是分子筛单独吸附 NO 后的 TPSR 谱. 可以看出, 在 315 °C 附近出现宽的 NO 脱附峰, 说明存在 NO 的强化学吸附. 图 3(b) 是分子筛共吸附 NO 和 $O_2$ 的 TPSR 谱. 与单独吸附 NO 相比, 分子筛上的 NO 脱附量明显增加, 与文献[6]结果一致, 且脱附温度范围更宽, 同时在 125 °C 出现 NO 脱附峰, 在 379 和 438 °C 处出现相互重叠的 NO 脱附峰, 而 315 °C 附近宽的 NO 脱附峰增强, 说明 $O_2$

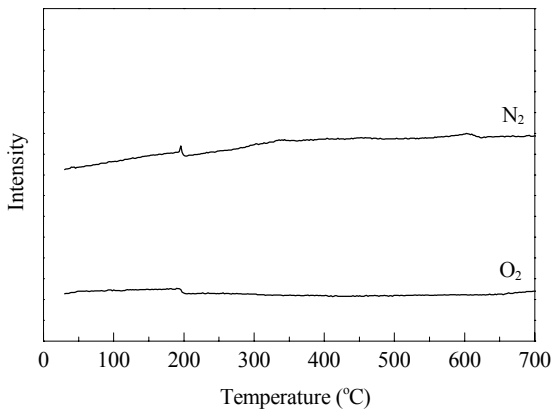


**图 2 Na-ZSM-5 单独吸附 $O_2$ 后的 TPSR 谱**

**Fig. 2.** TPSR profiles after adsorption of 20.7%$O_2$-79.3%$N_2$ on Na-ZSM-5 catalyst.

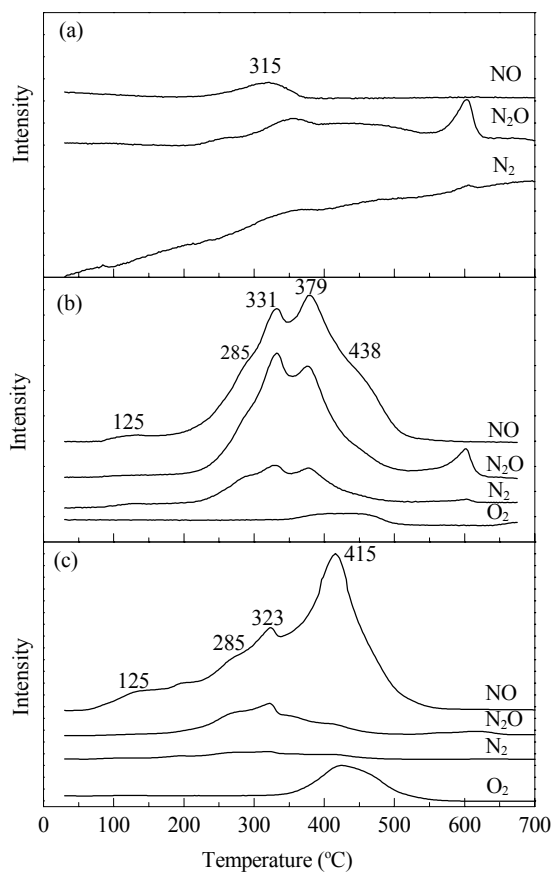


**图 3 Na-ZSM-5 上吸附不同 $NO_x$ 气体组分后的 TPSR 谱**

**Fig. 3.** TPSR profiles after adsorption of different gases on Na-ZSM-5 catalyst. (a) 0.05%NO-99.95%$N_2$; (b) 0.05%NO-20.7%$O_2$-79.25%$N_2$; (c) 0.05%$NO_2$-99.95%$N_2$.

的存在促进了 NO 的吸附. 刑娜等[13]认为, NO 与 $O_2$ 作用形成 $NO_2$, 可与 NO 共吸附在分子筛表面形成 $HNO_2$ 物种, 程序升温时会脱附出 NO 和 $NO_2$, 但本文中 NO-$O_2$ 的 TPSR 谱中并未检测到 $NO_2$, 即使单独吸附 $NO_2$ (图 3(c)) 也仍未检测到 $NO_2$, 所以推测大部分 $NO_2$ 在分子筛表面为物理吸附, 或者在升温过程中发生了 $NO_2$ 分解. 同时, 图 3(b) 中 125 和~315 °C 处宽的 NO 脱附峰与图 3(c) 相对应, 进一步说明图 3(b) 中这两处 NO 峰是 $NO_2$ 分解的产物. 图 3(b) 与 (c) 中在 400 °C 附近都同时出现 NO 和 $O_2$ 峰, 可能来源于同一 $NO_x$ 吸附物种, 即 NO 在分子筛上氧化为 $NO_2$ 中间体.

以上结果表明, NO 在 Na-ZSM-5 分子筛表面的氧化过程表现为类似 Eley-Rideal 反应机理, 即吸附的 NO 与气相中 $O_2$ 反应, 最终生成 $NO_2$.

图 3(a) 与 (b) 中出现的 $N_2O$ 峰推断为高温下 NO 分解所致. 每个 $N_2O$ 峰位置处都伴随着 $N_2$ 峰, 由于 $N_2$ 在催化剂表面不吸附, 排除了气相中 $N_2$ 的干扰, 因而该 $N_2$ 只能是 $N_2O$ 进一步分解所得[14].

### 2.3 Na-ZSM-5 分子筛上 NO 氧化反应体系的原位 DRIFTS 研究

图 4 为 30 °C 下 0.1% NO 在 Na-ZSM-5 上吸附过程的原位 DRIFTS 谱. 由图可见, 随着时间的延长, 所有峰都在不断增强. 其中, 3 000~3 700 $cm^{-1}$ 处一般归属于–OH 峰[15], 2 min 时该峰处于 3 250 $cm^{-1}$, 到 10 min 时位移至 3 300 $cm^{-1}$ 处并增强, 表明–OH 可能为 NO 吸附位. 3 300 和 2 900 $cm^{-1}$ 归属于分子筛桥式–OH 位上吸附 NO 引起的红外吸收振动峰. 2 010

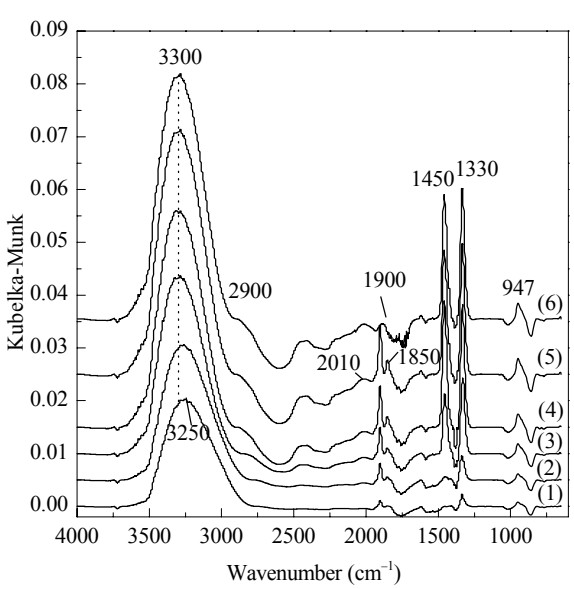


**图 4 Na-ZSM-5 分子筛上吸附 NO 的 DRIFTS 谱**

**Fig. 4.** DRIFTS spectra of NO adsorbed on Na-ZSM-5 catalyst. (1) 2 min; (2) 5 min; (3)10 min; (4) 15 min; (5) 20 min; (6) $N_2$ flushing after saturated adsorption.

$cm^{-1}$ 处是吸附态 NO 的振动峰[16]. 1 810~1 900 $cm^{-1}$ 处一般归属于金属离子吸附 NO 引起的振动峰[17,18], 因此, 1 850 和 1 900 $cm^{-1}$ 归属于 Na-ZSM-5 上 $Na^+$吸附位上的 NO 振动峰. Perdana 等[16]认为, 1 450 $cm^{-1}$ 处也为 $Na^+$吸附 NO 的振动峰. 待 NO 吸附饱和后, 用 $N_2$ 吹扫 10 min, 发现只有 1 900 和 1 850 $cm^{-1}$ 处的峰变弱或消失, 其它峰强度均不变, 说明 $Na^+$上吸附的 NO 同时存在强弱两种吸附形式, 而–OH 位上 NO 为较强吸附态.

图 5(a) 为 Na-ZSM-5 分子筛共吸附 NO 和 $O_2$ 饱和后的 DRIFTS 谱. 可以看出, 对应于图 4 中的 2 010, 1 900, 1 850, 1 450 和 1 330 $cm^{-1}$ 处峰全部消失, 说明这些活性位上吸附的 NO 都参与了氧化反应. 同时在 1 200~1 741 $cm^{-1}$ 处出现新峰, 其中, 1 600 $cm^{-1}$ 处峰最强, 为气相或弱吸附 $NO_2$[19]; 1 200 和 1 630 $cm^{-1}$ 归属于 $NO_2$ 的吸附振动峰[14,19]; 1 680 $cm^{-1}$ 归属于 $HNO_2$[15,20]; 1 260 和 1 310 $cm^{-1}$ 处峰分别归属于 NO[21]和 $NO_3$ 的振动峰[22], 而 1 741 $cm^{-1}$ 为 $N_2O_4$[23]. 说明 NO 氧化生成 $NO_2$ 的过程中, 同时形成了 $N_2O_4$ 和 $NO_3$ 等中间物种.

待吸附饱和后停止通入 NO 和 $O_2$, 用 $N_2$ 吹扫后样品的 DRIFTS 谱见图 5(b). 可以看出, 所有 $NO_2$ 峰 (1 200, 1 600 和 1 630 $cm^{-1}$) 均消失, 1 741 $cm^{-1}$ 处 $N_2O_4$ 峰也大大减弱, 说明 $NO_2$ 和 $N_2O_4$ 在 Na-ZSM-5 上主要以弱吸附形式存在. 另外, 弱吸附态的 NO 峰 (1 260 $cm^{-1}$) 也消失, 而 $NO_3$ 振动峰 (1 310 $cm^{-1}$) 仍存在. 1 608 和 1 470 $cm^{-1}$ 处出现新的归属于 $NO_3$ 的吸收峰[15,16], 表明 NO 和 $NO_2$ 脱附留下的空位可能为 $NO_3$ 重新吸附而被占据.

利用 DRIFTS 谱研究了不同温度下 Na-ZSM-5 上 NO 和 $O_2$ 的共吸附, 结果见图 6. 由图可见, 在 30 °C 下通入含 0.1 %NO 和 20.7 %$O_2$ 的混合气, 待吸附饱和后用 $N_2$ 吹扫除去分子筛表面气相分子, 可以观察到 3 300 (–OH), 1 741 ($N_2O_4$), 1 680 ($HNO_2$), 1 608, 1 470, 1 310 ($NO_3$) 以及 947 $cm^{-1}$(NO) 等红外振动峰; 当温度升至 90 °C 时, 1 741 和 1 680 $cm^{-1}$ 处的红外峰消失, 而其余的峰都稍有减弱; 至 150 °C 时, 1 608 和 947 $cm^{-1}$ 峰几乎消失, 只剩下 1 470 和 1 310 $cm^{-1}$ 处的红外峰, 为强吸附态 $NO_3$, 而 3 300 $cm^{-1}$ 处的峰减弱并移至 3 370 $cm^{-1}$. 当温度升至 300 °C 时, 3 370 和 1 470 $cm^{-1}$ 峰明显减弱, 而 1 310 $cm^{-1}$ 处出现肩峰 (1 300 $cm^{-1}$) 并增强, 可能是 $NO_3$ 开始分解生成新的物质. 当温度为 400 °C 时, 1 300 $cm^{-1}$ 处峰继续增强, 并出现明显的 $O_2$ 峰 (1 011 $cm^{-1}$). 结合 NO-$O_2$-TPSR 谱中~400 °C 会有 NO 和 $O_2$ 生成, 推断此温度下分解生成的 NO 和 $O_2$ 来源于 $NO_3$, 遵循反应式 $NO_3(s) \rightarrow$

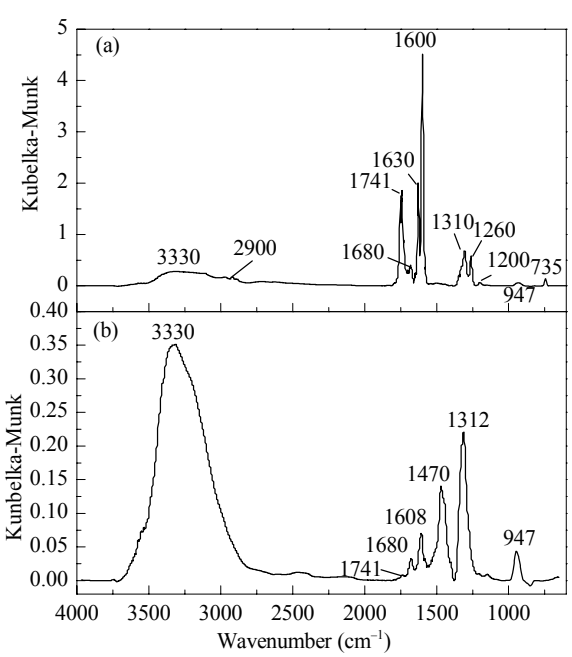


**图 5 Na-ZSM-5 分子筛上共吸附 NO 和 $O_2$ 的 DRIFTS 谱**

**Fig. 5.** DRIFTS spectra of NO and $O_2$ co-adsorption on Na-ZSM-5 catalyst (a) before $N_2$ flushing; (b) after $N_2$ flushing.

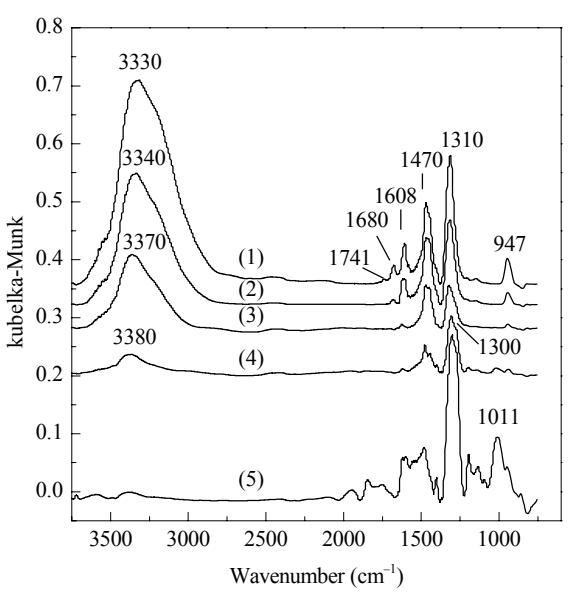


**图 6 不同温度下 Na-ZSM-5 分子筛上吸附 NO 和 $O_2$ 的 DRIFTS 谱**

**Fig. 6.** DRIFTS spectra of NO and $O_2$ co-adsorption over Na-ZSM-5 at different temperatures. (1) 30 °C; (2) 90 °C; (3) 150 °C; (4) 300 °C; (5) 400 °C.

$NO(s)+O_2$.

综合考虑 NO 和 $O_2$ 共吸附后的 DRIFTS 和 TPSR 谱可知, NO 氧化生成的 $NO_2$ 及 $N_2O_4$ 在分子筛上大部分是以弱吸附态或气态存在, 经 $N_2$ 吹扫即发生脱附; 而小部分可转化成强吸附态的 $NO_3$, 在高温下分解成 NO 和 $O_2$ 而脱附. 因此在分子筛共吸附 NO 和 $O_2$ 的 TPSR 谱中检测不到 $NO_2$.

### 2.4 NO吸附-氧化过程机理分析

综上可知, 常温下 NO 和 $O_2$ 在分子筛表面反应后形成 $NO_2$, $N_2O_4$, $NO_3$ 和 NO 等中间物种. 根据这些中间物种的形成及吸附强度, 可以推测 NO 和 $O_2$ 在高硅 Na-ZSM-5 分子筛上的反应机理为: NO 首先吸附在分子筛活性位上, 吸附态 NO 与气相中的 $O_2$ 反应生成吸附态 $NO_3$, 然后进一步与吸附态 NO 作用转化为 $NO_2$ 和 $N_2O_4$, 如图式 1 所示.

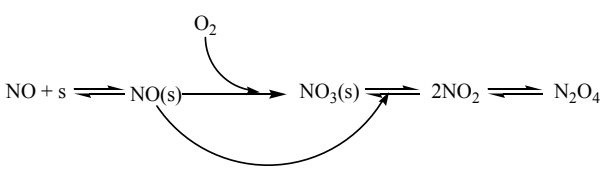


**图式 1 高硅 Na-ZSM-5 分子筛上 NO 氧化反应机理**

**Scheme 1.** Mechanism of NO oxidation over high silica Na-ZSM-5 molecular sieves.

在反应开始阶段, NO 的吸附及其与 $O_2$ 的反应为主要过程, 生成强吸附态 $NO_3$, 并继续与吸附的 NO 反应生成弱吸附态的 $NO_2$ 和 $N_2O_4$, 此时无 $NO_2$ 释放, NO 出口浓度变化不大, 相当于图 1 中 0~15 min 这一时间段. 随着反应的进行, Na-ZSM-5 表面 $NO_2$ 和 $N_2O_4$ 的吸附量逐渐增加, 上述反应受到抑制, 此时 NO 出口浓度缓慢增加, 相当于图 1 中 15~60 min 时间段, 为第二过程. 随着 $NO_2$ 吸附饱和而释放, 又进一步促进了 NO 与 $NO_3$ 的反应, NO 出口浓度急剧下降, 上述两个过程同时进行, 相互作用, 最终达到吸附-氧化动态平衡. 此机理解释了 NO 和 $O_2$ 氧化过程中的瞬态变化曲线, 以及 NO-$O_2$-TPSR 和 $NO_2$-TPSR 中没有检测到 $NO_2$、分子筛表面吸附态 $NO_3$ 在高温下分解形成 NO 和 $O_2$ 等现象.

## 3 结论

常温下高硅 Na-ZSM-5 分子筛具有催化氧化 NO 的性能, 主要吸附活性位是–OH 和 $Na^+$, 在催化氧化 NO 的过程中, 大部分 $NO_2$ 在分子筛上是以物理吸附的形式存在. NO 和 $O_2$ 的反应机理为: NO 首先吸附在分子筛活性位上, 化学吸附的 NO 与气相 $O_2$ 反应生成吸附的 $NO_3$, 并继续与吸附的 NO 作用转化成 $NO_2$ 和 $N_2O_4$, 当其达到饱和吸附后释放出来, 从而达到吸附-氧化的动态平衡; 强吸附的 $NO_3$ 在 NO 氧化过程中起到中间体的作用, 同时也促进了 NO 的吸附.

## 参 考 文 献


1 Goo J H, Irfan M F, Kim S D, Hong C H. *Chemosphere*, 2007, **67**: 718
2 Koebel M, Madia G, Elsener M. *Catal Today*, 2002, **73**: 239
3 Thomas D, Vanderschuren J. *Sep Purif Technol*, 2000, **18**: 37
4 de Paiva J L, Kachan G C. *Chem Eng Process*, 2004, **43**: 941
5 袁从慧, 刘华彦, 卢晗锋, 李玉芳, 陈银飞. 化学反应工程与工艺 (Yuan C H, Liu H Y, Lu H F, Li Y F, Chen Y F. *Chem Reac Eng Technol*), 2008, **24**: 476
6 袁从慧, 刘华彦, 卢晗锋, 李玉芳, 陈银飞. 环境工程学报 (Yuan C H, Liu H Y, Lu H F, Li Y F, Chen Y F. *Chin J Environ Eng*), 2008, **2**: 1207
7 Despres J, Koebel M, Krocher O, Elsener M, Wokaun A. *Microporous Mesoporous Mater*, 2003, **58**: 175
8 Gomez-Garcia M A, Pitchon V, Kiennemann A. *Environ Int*, 2005, **31**: 445
9 Perdana I, Creaser D, Ohrman O, Hedlund J. *Appl Catal B*, 2007, **72**: 82
10 Shi C, Cheng M J, Qu Z P, Bao X H. *J Mol Catal A*, 2005, **235**: 35
11 Guo Zh Ch, Xie Y Sh, Hong I, Kim J. *Energy Convers Manage*, 2001, **42**: 2005
12 李玉芳, 刘华彦, 黄海凤, 张泽凯, 陈银飞. 中国环境科学 (Li Y F, Liu H Y, Huang H F, Zhang Z K, Chen Y F. *China Environ Sci*), 2009, **295**: 469
13 邢娜, 王新平, 于青, 郭新闻. 催化学报 (Xing N, Wang X P, Yu Q, Guo X W. *Chin J Catal*), 2007, **28**: 205
14 Devadas M, Krocher O, Elsener M, Wokaun A, Soger N, Pferfer M, Demel Y, Mussmann L. *Appl Catal B*, 2006, **67**: 187
15 Kantcheva M, Vakkasoglu A S. *J Catal*, 2004, **223**: 352
16 Perdana I, Creaser D, Öhrman O, Hedlund J. *J Catal*, 2005, **234**: 219
17 Lobree L J, Hwang I C, Reimer J A, Bell A T. *J Catal*, 1999, **186**: 242
18 Hadjiivanov K, Knozinger H, Tsyntsarski B, Dimitrov L. *Catal Lett*, 1999, **62**: 35
19 Milushev A, Hadjiivanov K. *Phys Chem Chem Phys*, 2001, **3**: 5337
20 Brosius R, Bazin P, Thibault-Starzyk F, Martens J A. *J Catal*, 2005, **234**: 191
21 Szanyia J, Kwaka J H, Burtonb S, Rodriguez J A, Peden C

H F. *J Electron Spectrosc Relat Phenom*, 2006, **150**: 164
22 柯锐, 李俊华, 郝吉明, 傅立新, 陈强, 赵大庆. 催化学报 (Ke R, Li J H, Hao J M, Fi L X, Chen Q, Zhao D Q. *Chin J Catal*), 2005, **26**: 951
23 Hadjiivanov K, Klissurski D , Ramis G, Busca G. *Appl Catal B*, 1996, **7**: 251

## 英 译 文
## *English Text*

The abatement of nitric oxides ($NO_x$) is an important challenge because $NO_x$ compounds are a source of severe eco-environmental problems and are harmful to human health. Selective catalytic reduction (SCR), absorption, and adsorption are widely applied in the $NO_x$ emission control area. To increase the removal efficiency of $NO_x$, it is beneficial to maintain a high ratio of $NO_2/NO_x$ in the feed. Goo et al. [1] concluded that the presence of $NO_2$ enhances the SCR activity at lower temperature and the optimum ratio of $NO_2/NO_x$ was found to be 0.5 for the $V_2O_5$-$WO_3$-$MnO_2/TiO_2$ catalyst in the $NH_3$-SCR process. Koebel et al. [2] obtained similar results, that is, equimolar amounts of NO and $NO_2$ led to the highest $NO_x$ conversion over the $V_2O_5$-$WO_3/TiO_2$ catalyst. For absorption by alkaline aqueous solutions, a high $NO_2/NO_x$ ratio is required to obtain high $NO_x$ removal efficiency. Generally, a 0.5–0.6 fraction of $NO_2$ in $NO_x$ is required during the NaOH solution absorption process since $NO_x$ compounds are removed primarily by the formation of $N_2O_3$ from the reaction of NO with $NO_2$ [3–5]. Furthermore, the required fraction would be much higher if a $(NH_4)_2SO_3$-NaOH solution was used for absorption because the reduction of $(NH_4)_2SO_3$ with $NO_2$ is much stronger than that with NO [6]. Because NO has difficultly adsorbing onto the surface of adsorbents, NO has to be oxidized to $NO_2$ first and then a high adsorption volume can be obtained [7]. Unfortunately, the $NO_x$ in power station or industrial plant exhaust gases typically consist of more than 90% NO [8], which means that the fractional oxidation of NO to $NO_2$ is a key step in all $NO_x$ abatement processes.

Many studies have been done on ZSM-5 molecular sieves and ion-exchanged ZSM-5, which is used for $NO_x$ adsorption and reduction [9,10]. Only a few of these studies have focused on NO oxidation, especially at ambient temperature. Instead, activated carbon (AC) and active carbon fiber (ACF) have widely been reported to be used as catalysts for NO oxidation. AC and ACF, however, have a high adsorption volume for vapor, which is preferred over $NO_x$ absorption and this leads to low catalytic activity for NO oxidation and limits their application in industry [11]. Accordingly, a highly hydrophobic surface can be obtained on molecular sieves with a high Si/Al ratio and our early research emphasized the high silica content ZSM-5 molecular sieve for NO oxidation. The results confirmed that far higher catalytic activity can be obtained for ZSM-5 than for AC or ACF under high vapor conditions [12], which means that the ZSM-5 catalyst has potential industrial application. Based on these results, for this paper we focused on the reaction pathway between NO and $O_2$, and also on the species adsorbed on the surface of the high silica content Na-ZSM-5. Furthermore, we discuss the reaction mechanism. We hope that this work provides a theoretical direction for the improvement of catalytic activity and for the study of the reaction kinetics of ZSM-5.

## 1 Experimental

### 1.1 Catalyst treatment and the adsorption-reaction test

Na-ZSM-5 ($SiO_2/Al_2O_3$ molar ratio of 300) was provided by Shanghai Zhuoyue Chemicals Co., Ltd. The methods used for catalyst treatment and the reaction test have been reported in Ref. [12]. The main operation conditions in the adsorption-reaction tests were as follows: catalyst loading 3.7 g; molar fraction of NO and $O_2$ of 0.05% and 20.7%, respectively, in the inlet $NO_x$ mixed gas with $N_2$ as the balance; total flow rate 2 L/min; reaction temperature 30 °C. The concentrations of NO and $NO_2$ in the gas stream were measured using a Testo 350-XL flue gas analyzer.

### 1.2 Catalyst characterization

Temperature-programmed surface reaction (TPSR): the Na-ZSM-5 molecular sieves were flushed by a $N_2$ gas stream at 500 °C for 2 h and then cooled down to a specific temperature that varied from 30 °C to 400 °C. This was followed by the adsorption of a mixed gas with different components including 20.7%$O_2$-79.3%$N_2$, 0.05%NO-99.95%$N_2$, 0.05% NO-20.7%$O_2$-79.25%$N_2$, 0.05%$NO_2$-99.95%$N_2$ etc. The outlet concentrations of NO and $NO_2$ were measured using a Testo 350-XL flue gas analyzer. After saturated adsorption was obtained, the surface of the catalyst was flushed with a $N_2$ gas stream again to remove the weakly adsorbed surface species. Finally, temperature programmed desorption was done at a heating rate of 10 °C/min from 30 °C to 600 °C and the desorbed species were detected using the Omini-Star mass spectrometer.

The reaction of NO and $O_2$ on the surface of Na-ZSM-5 was further investigated using a VENTEX 70 infrared spectrometer equipped with a MCT detector at a resolution of 4 $cm^{-1}$ (128 scans). The Na-ZSM-5 powders were first placed in a diffuse in situ cell, flushed with a $N_2$ gas stream at 400 °C for 2 h and then cooled to the specific reaction temperature. The diffuse IR spectra of the Na-ZSM-5 catalyst were first

measured at different temperatures as the corresponding reference, and then a mixed gas with different components was introduced into the in situ cell for adsorption and reaction. The diffuse reflectance infrared Fourier transform spectroscopy (DRIFTS) spectra were recorded at regular time intervals.

## 2 Results and discussion

### 2.1 Transient profiles of the NO catalytic oxidation on the Na-ZSM-5 molecular sieves

The trend of outlet NO and $NO_2$ concentrations with time is shown in Fig. 1. As soon as the $NO_x$ mixed gas passed through the reactor, NO was detected in the outlet but the concentration of NO was less than that in the inlet and the $NO_2$ concentration was too low to be detected in the first period, which means that adsorption takes place on the surface of ZSM-5. With time, the outlet NO concentration increased slowly until it reached 60 min on stream upon which it decreased sharply. At the same time, the outlet concentration of $NO_2$ began to increase sharply. Finally, the adsorption-reaction process reached a steady state at around 65 min when the outlet concentration of $NO_x$ was equal to that of the inlet. On the contrary, for the blank experiment where the reactor was used without ZSM-5 catalyst packing under the same operating conditions, a steady state was reached within 5 min and the outlet NO concentration was 0.0497% (equal to that of inlet). Therefore, the oxidation of NO can be neglected in the blank reactor. These experiments prove that the Na-ZSM-5 molecular sieve shows a catalytic effect toward NO oxidation by $O_2$ at ambient temperature.

### 2.2 TPSR measurements of NO oxidation over Na-ZSM-5

Figure 2 shows TPSR profiles of the $O_2$ and $N_2$ adsorbed on Na-ZSM-5. No oxygen was detected during the TPSR and this is possibly because of $O_2$ not adsorbing on Na-ZSM-5. Figure 3 shows TPSR profiles for the saturated adsorption of $NO_x$ on Na-ZSM-5. A desorption peak is present at 315 °C in the TPSR profile of individually adsorbed NO on Na-ZSM-5 (Fig. 3(a)), which means that there exists NO adsorption strongly. Figure 3(b) shows the TPSR profile of $NO/O_2$ co-adsorption. Similar to the phenomena in Ref. [6], the amount of NO released during TPSR increased remarkably compared to that of single NO adsorption. The intensity of the peak at 315 °C increased and more NO desorption peaks appeared at 125, 379, and 438 °C. The latter two peaks overlap because of the wider temperature range. The presence of $O_2$ in the mixed $NO_x$ gas promotes NO adsorption on Na-ZSM-5. Xing et al. [13] postulated that $NO_2$ from the reaction of NO with $O_2$ could co-adsorb with NO on the surface of Na-ZSM-5 and form a $HNO_2$ specie, which would desorb from the surface of Na-ZSM-5 by the form of NO and $NO_2$ during the followed TPD program. In our study, $NO_2$ was not detected during the TPSR measurement of $NO/O_2$ co-adsorption and $NO_2$ single adsorption (Fig. 3(c)) so we conclude that $NO_2$ exists on the surface of Na-ZSM-5 through the physical adsorption. The possibility of $NO_2$ decomposition during TPSR should, however, not be ignored. Nevertheless, the desorption peaks at 125 and ~315 °C are present in Fig. 3(b) and in Fig. 3(c), which means that these desorbed species originate from the products of $NO_2$ decomposition. From Fig. 3(b) and 3(c), both the NO and $O_2$ desorption peaks exist simultaneously at 400 °C and they might originate from the same adsorbed species, i.e., the intermediate from the reaction of NO to $NO_2$ conversion on the surface of Na-ZSM-5.

From the TPSR measurements, the oxidation process of NO by $O_2$ on the surface of Na-ZSM-5 followed the Eley-Rideal reaction mechanism, that is, the adsorbed NO reacts with gaseous $O_2$ and forms $NO_2$.

In addition, the desorbed $N_2O$ species at 315 and 379 °C probably originate from the decomposition of NO at high temperature. Also, the release of $N_2$ accompanied by $N_2O$ comes from the further decomposition of $N_2O$ [14] because $N_2$ does not adsorb on Na-ZSM-5 according to Fig. 2.

### 2.3 In situ DRIFTS characterization of NO oxidation on Na-ZSM-5

Figure 4 shows the in situ DRIFTS spectra of the adsorption process for 0.1% NO on Na-ZSM-5. With an increase in the adsorption time, the strength of all the adsorption peaks increased. The strongest peak changed from 3 250 to 3 300 $cm^{-1}$ and the intensity increased continuously, which indicates that the –OH group on the surface of Na-ZSM-5 might be an adsorption site for NO since the peaks at 3 000–3 700 $cm^{-1}$ are usually assigned to species adsorbed on –OH sites [15]. The peaks at 3 300 and 2 900 $cm^{-1}$ are assigned to the IR vibration of adsorbed NO on the bridge-linked –OH group of Na-ZSM-5. The peak at 2 010 $cm^{-1}$ is assigned to the vibration of adsorbed NO [16]. The adsorption peaks at 1 450, 1 850, and 1 900 $cm^{-1}$ are associated with the IR vibration of adsorbed NO on the $Na^+$ site of the Na-ZSM-5 molecular sieve [16–18]. When Na-ZSM-5 is flushed for 10 min using a $N_2$ stream after the saturated adsorption of NO, we found that only the peaks at 1 900 and 1 850 $cm^{-1}$ weakened and even disappeared, as shown in Fig. 4(6), which indicates that two types of the adsorption sites exist simultaneously on the surface of Na-ZSM-5, i.e., one is a strong adsorption site and the other a weak one. The –OH group would be associated with the stronger one.

Figure 5(a) shows the DRIFTS spectra for saturated $NO/O_2$ co-adsorption on Na-ZSM-5. From the spectra, we found that the peaks at 2 010, 1 900, 1 850, 1 450, and 1 330 $cm^{-1}$ in Fig. 4 disappeared, which suggests that all the adsorbed NO on these sites took part in the oxidation reaction. At the same time, new peaks appeared between 1 200–1 741 $cm^{-1}$ including the strongest peak at 1 600 $cm^{-1}$, which is assigned to gaseous or weakly adsorbed $NO_2$ [19], the adsorption vibration of $NO_2$ at 1 200 and 1 630 $cm^{-1}$ [14,19], $HNO_2$ at 1 680 $cm^{-1}$ [15,20], the vibration of NO [21] and $NO_3$ [22] at 1 260 and 1 310 $cm^{-1}$, respectively as well as $N_2O_4$ at 1 741 $cm^{-1}$ [23]. From this data, $N_2O_4$ and $NO_3$ adsorbed species are obviously formed during the oxidation reaction of NO to $NO_2$.

After saturation of the $NO/O_2$ adsorption, Na-ZSM-5 was flushed with $N_2$ gas, and IR spectra were recorded at different times. Compared to the spectra in Fig. 5(a), all the $NO_2$ peaks at 1 200, 1 600, and 1 630 $cm^{-1}$ disappeared and the $N_2O_4$ peak at 1 741 $cm^{-1}$ weakened, as shown in Fig. 5(b), which means that the adsorption of $NO_2$ and $N_2O_4$ on the surface of Na-ZSM-5 is because of a weak physical adsorption. Although the weakly adsorbed NO peak at 1 260 $cm^{-1}$ also disappears, the $NO_3$ vibration peak at 1 310 $cm^{-1}$ still exists. Nevertheless, after flushing with a $N_2$ stream, the new IR peaks at 1 608 and 1 470 $cm^{-1}$ are assigned to the adsorbed $NO_3$ species [15,16]. This might originate from vacant sites that result from NO and $NO_2$ desorption. Therefore, the $NO_3$ species might originate from strong adsorption on Na-ZSM-5.

The effects of temperature on the co-adsorption of $NO/O_2$ on Na-ZSM-5 were further investigated using in situ DRIFTS. First, the mixed gas containing 0.1% NO and 20.7% $O_2$ was introduced into the diffuse in situ cell. When saturated adsorption was reached, Na-ZSM-5 was flushed using a $N_2$ gas stream and gradually heated. The IR spectra are shown in Fig. 6. When the temperature was kept at 30 °C, peaks were present at 3 300 (NO), 1 741 ($N_2O_4$), 1 680, 1 470, 1 310 ($NO_3$), and 947 $cm^{-1}$ (NO). When the temperature was increased to 150 °C, the peaks at 1 741 and 1 680 (90 °C), 1 608 and 947 $cm^{-1}$ (150 °C) disappeared in this sequence and only the peaks at 1 470 and 1 310 $cm^{-1}$ that are assigned to the strongly adsorbed $NO_3$ species are left. The peak at 3 300 $cm^{-1}$ decreased in intensity and blue-shifted to 3 370 $cm^{-1}$. When the temperature was increased to 300 °C, the peaks at 3 370 and 1 470 $cm^{-1}$ weakened significantly. Conversely, the peak at 1 310 $cm^{-1}$ accompanied by the shoulder peak at 1 300 $cm^{-1}$ strengthened, which means that a new specie was formed from the reaction of $NO_3$. When the temperature increased to 400 °C, the peak at 1 300 $cm^{-1}$ continued to strengthen and an intensive peak was present at 1 101 $cm^{-1}$ and is assigned to $O_2$. Based on these results, it is inferred that the newly formed NO and $O_2$ originated from the decomposition of the adsorbed $NO_3$ intermediate according to the following equation: $NO_3(s) \rightarrow NO(s) + O_2$.

Furthermore, according to TPSR and DRIFTS characterization of the $NO/O_2$ co-adsorption, most of the $NO_2$ and $N_2O_4$ formed by the oxidation of NO were weakly physically adsorbed on the Na-ZSM-5 molecular sieve or existed in the gas phase and, therefore, were easily desorbed or flushed out by $N_2$. The others were converted into strongly adsorbed $NO_3$ species, which decomposed further into NO and $O_2$ and then desorbed from the surface of Na-ZSM-5 at high temperature. Therefore, $NO_2$ was hardly detected in the TPSR spectra for $NO/O_2$ co-adsorption.

### 2.4 Analysis of the adsorption-oxidation reaction mechanism of NO by $O_2$

From the study of DRIFTS and TPSR, some intermediates such as $NO_2$, $N_2O_4$, and $NO_3$ obviously formed during the surface reaction of NO with $O_2$ on Na-ZSM-5 at ambient temperature. Based on these results, the adsorption and reaction pathway of NO with $O_2$ on the surface of Na-ZSM-5 was further analyzed. First, gaseous NO is adsorbed on the surface of Na-ZSM-5 chemically and then the adsorbed NO species reacts with gaseous $O_2$ to form chemically adsorbed $NO_3$, which reacts with adsorbed NO and transforms into $NO_2$ and $N_2O_4$. A detailed adsorption reaction mechanism of NO with $O_2$ is shown in Scheme 1.

At the beginning of the NO oxidation reaction, the main behavior is NO adsorption and then reaction with gaseous $O_2$. The adsorbed $NO_3$ from the NO oxidation continues to react with adsorbed NO to give $NO_2$ and $N_2O_4$, which physically adsorb onto Na-ZSM-5 with a high adsorption volume and $NO_2$ is not released during this period. This stage corresponds to 0–15 min as shown in Fig. 1. NO oxidation in the first stage is constrained as the reaction progresses and the concentration of NO in the outlet increases slowly because the amount of $NO_x$ adsorption, especially $NO_2$ adsorption, on Na-ZSM-5 kept increasing. This period is the second stage and corresponds to 15–60 min, as shown in Fig. 1. When $NO_2$ reaches the saturated adsorption stage and is released, the vacant adsorption sites increase and the reaction of $NO_3$ with NO increases leading to a sharp decrease in the outlet NO concentration. Finally, the whole process reaches a dynamic equilibrium state between $NO_2$ desorption and the reaction of NO. This adsorption-reaction mechanism explains the transient profiles in the oxidation reaction pathway of NO with $O_2$ over Na-ZSM-5, as shown in Fig. 1. It also explains why $NO_2$ was not be detected in the outlet for $NO$-$O_2$-TPSR and $NO_2$-TPSR and the process for $NO_3$ adsorption on the surface of Na-ZSM-5 as well as the decomposition into NO and $O_2$ at high temperature.

## 3 Conclusions

High silica content Na-ZSM-5 molecular sieves exhibit high catalytic activity at ambient temperature because of the active adsorption sites consisting of –OH groups and $Na^+$ ions. During the catalytic oxidation of NO by $O_2$, Na-ZSM-5 weakly adsorbs $NO_2$, which mainly physically adsorbs on the surface. The oxidation reaction mechanism of NO with $O_2$ can be explained as follows: (1) chemical adsorption of NO onto the surface of Na-ZSM-5 and the formation of chemically adsorbed $NO_3$ by the reaction of adsorbed NO and gaseous $O_2$; (2) The formation and sequential physical adsorption of $NO_2$ and $N_2O_4$ by the reactions of NO and $NO_3$; (3) the release of $NO_2$ and $N_2O_4$ after saturated adsorption and a subsequent reaction-adsorption dynamic equilibrium. The strong adsorption of $NO_3$ acts as an intermediate for NO oxidation by $O_2$ and NO adsorption is also improved.

***Full-text paper available online at ScienceDirect***
***http://www.sciencedirect.com/science/journal/18722067***